Gondwana Research 16 (2009) 622–632

Contents lists available at ScienceDirect

Gondwana Research

journal homepage: www.elsevier.com/locate/gr

Ordovician ferrosilicic magmas: Experimental evidence for ultrahigh temperatures affecting a metagreywacke source

A. Castro [a,*], A. García-Casco [b], C. Fernández [c], L.G. Corretgé [d], I. Moreno-Ventas [a], T. Gerya [e], I. Löw [e]

[a] Departamento de Geología, Universidad de Huelva, Campus del Carmen, 21071 Huelva, Spain
[b] Departamento de Mineralogía y Petrología, Instituto Andaluz de Ciencias de la Tierra, Universidad de Granada-CSIC, Avenida Fuentenueva sn, 18002 Granada, Spain
[c] Departamento de Geodinámica y Paleontología, Universidad de Huelva, Campus del Carmen, 21071 Huelva, Spain
[d] Departamento de Geología, Universidad de Oviedo, Arias de Velasco, s/n, Oviedo Spain
[e] Department of Earth Sciences, ETH Zurich, Clausiusstrasse 25, CH-8092, Zurich, Switzerland

ARTICLE INFO

Article history:
Received 11 September 2008
Received in revised form 17 December 2008
Accepted 18 December 2008
Available online 1 January 2009

Keywords:
Ferrosilicic magmatism
Experimental petrology
Mantle-wedge plumes
Gondwana
Cambro-Ordovician
Crustal recycling

ABSTRACT

Peculiar magmatic rocks were erupted and emplaced at depth at the margin of the Gondwana supercontinent during the Cambro-Ordovician transition. These rocks are characterized by high contents in silica and iron but they do not have equivalents in the high-silica members of the calc-alkaline series. They have particular geochemical signatures, with Al saturation index, ASI >1, FeO>2.5 wt.%, MgO>0.8 wt.% for very low contents in calcium (CaO<2.0 wt.%), supporting a derivation from near-total melting (>80 vol.% melt) of metagreywackes. The results from inverse experiments indicate that the most plausible conditions are within the range 1000 °C (excess water) and 1100–1200 °C (subsaturated and dry) at pressures of 1.5 to 2.0 GPa. A tectonic scenario implying melting of subducted sediments within an ascending mantle-wedge plume is suggested for the generation of primary ferrosilicic melts at the Gondwana continental margin during Upper Cambrian to Lower Ordovician times.

1. Introduction

The generation of silicic (SiO_2>63 wt.%) magmatic rocks of dacite to rhyolite compositions (and their plutonic equivalents) is directly related to the differentiation and evolution of the continental crust (Taylor and McLennan, 1985; Condie, 1997). Recycling of older crustal materials, either sedimentary or igneous, into silicic magmatism is widely supported by isotope geochemistry (McCulloch and Wasserburg, 1978; Allègre and Ben Othman, 1980) and laboratory experiments (Thompson, 1982; Vielzeuf and Holloway, 1988; Patiño Douce, 1999). However, only a little part of the silicic magmas may be produced at conditions predicted by currently accepted thermal models for the continental crust. With the exception of anatectic leucogranites, which may be produced from metasedimentary sources at temperatures of the order of 650 to 800 °C and middle crustal pressures (0.5 to 1.0 GPa), most of the silicic magmas need higher temperatures out of the range predicted by crustal thermal models.

Here we report a particular case of ferrosilicic magmatic rocks developed at the Gondwana margin at conditions exceeding any thermal model prediction for the continental crust. The peculiar geochemical features of these magmatic rocks, together with melting experiments supporting a derivation form metagreywackes, were reported in a previous paper (Fernández et al., 2008). In this study we show a complementary experimental proof derived from the application of inverse techniques to a model magma composition representing averaged Ordovician ferrosilicic magmas form Iberia. The aim of this study is to explore experimentally the near-liquidus phase relations for this particular system in order to produce an estimate of the required pressure and temperature conditions at which these particular liquids are segregated. This estimation will be independent of the source composition and it will be used to test the previous results from partial melting experiments (Fernández et al., 2008).

The application of alternative thermal models is also explored here in order to find a plausible scenario for magma generation at ultrahigh temperature in an active continental margin. Currently accepted models that have been proposed to account for thermal anomalies in the continental crust, including those of lithosphere delamination (Platt and England, 1993; Willner et al., 2002) and basaltic underplating (Petford and Atherton, 1996; Annen and Sparks, 2002) are not enough to account for the mantle-like thermal conditions required according to the experimental study. The solution to this paradox, recycling of continental rocks (metagreywackes) but not within the continental crust, requires the introduction and heating of sedimentary reservoirs into the hot mantle at temperatures higher than those predicted by thermal models in the continental crust. Near-total melting (>80 vol.% melt) also requires that progressive melt extraction from the source does not take place during melting, as it typically happens in the continental crust, where melting is commonly

* Corresponding author.
E-mail address: dorado@uhu.es (A. Castro).

1342-937X/$ – see front matter
doi:10.1016/j.gr.2008.12.011

accompanied by tectonic deformation (e.g., Brown, 1994). A plausible model accounting for recycling of crustal materials at ultra-high temperature (>1000 °C) within a closed system is offered by silicic cold plumes ascending through the mantle wedge (Gerya and Yuen, 2003; Gerya and Stoeckhert, 2005). These may transport fertile materials, dragged by subduction erosion (von Huene and Schöll, 1991) at the continental margin, to hot areas of the mantle wedge. The application of these models to the generation of ferrosilicic magmas is followed in this paper.

2. Geological setting and features of ferrosilicic magmatic rocks (FMR)

The rocks studied are characterized by high Fe and Mg contents (FeO>2.5 wt.%, MgO>0.8 wt.%), high silica values ranging from 65 to 70 wt.% SiO_2, and very low CaO (<2.0 wt.% CaO). Therefore, the term *ferrosilicic* is used in this paper to refer to these rocks, which are poorer in Ca than normal dacites and richer in Fe than normal rhyolites. The identification of these ferrosilicic rocks as derived from crystallisation

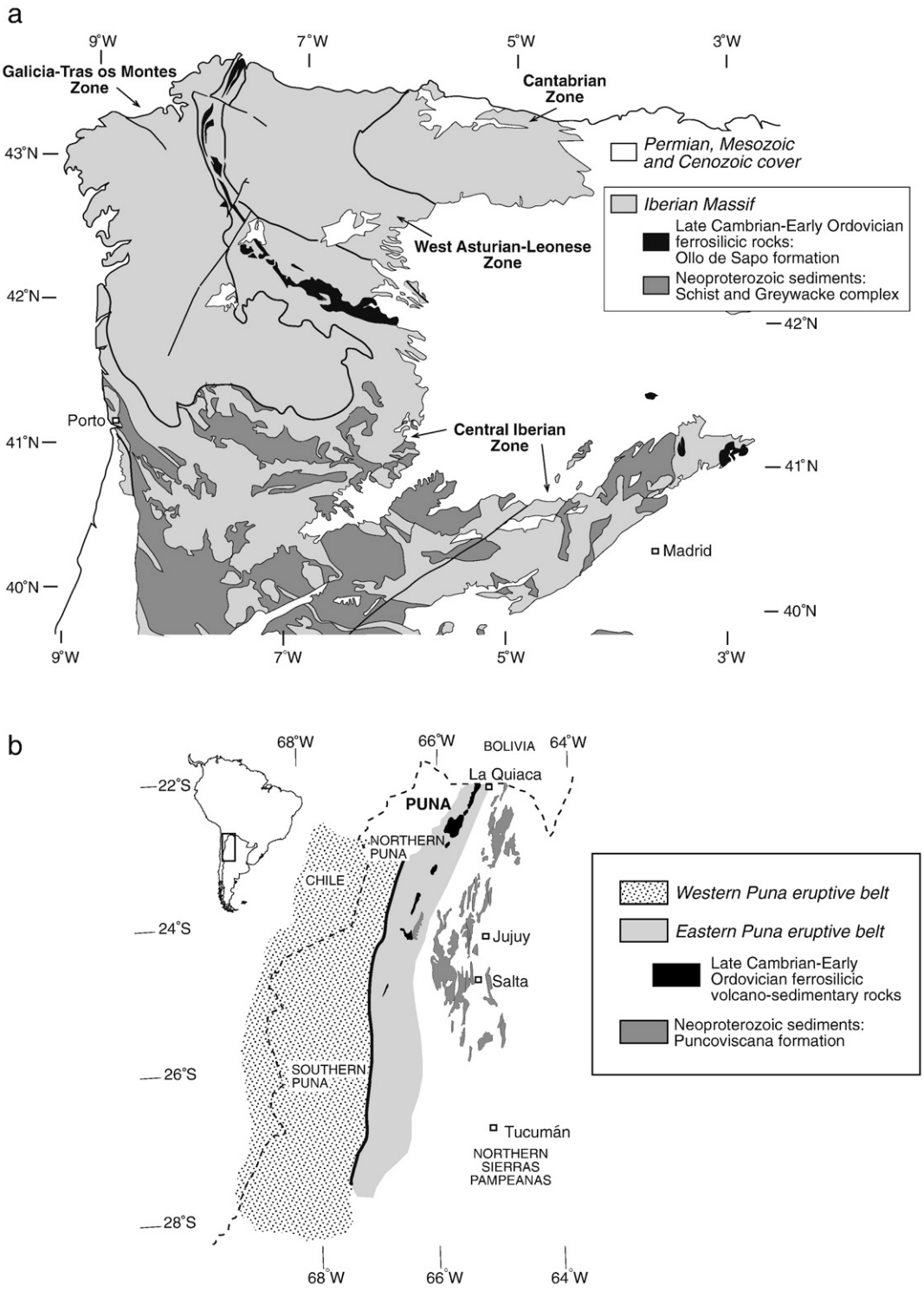

Fig. 1. Geological sketch map of (a) northwest Iberia and (b) northwestern Argentina.

of ferrosilicic magma requires a detailed observation of geological and textural features. In the Variscan Iberian massif (Iberia) and Puna (Argentina), the ferrosilicic magmatic rocks (FMR) form a thick sequence (several km in thickness) in which predominant eruptive rocks, but also subvolcanic and plutonic facies can be identified. FMR are represented in the Variscan Iberian massif by the so-called Ollo de Sapo formation (Parga Pondal et al., 1964). This unit is exposed along the core of a large anticlynorium at the northwestern part of the Iberian massif (Fig. 1a). The Ollo de Sapo formation is mostly comprised of gneisses, although less deformed and metamorphosed volcanic tuffs, ignimbrites and volcanoclastic facies have also been described (e.g., Díez Montes, 2007). Gneissose rocks show K-feldspar megacrysts (≤10–15 cm), blue quartz crystals and Na-rich (An_{5-15}) plagioclase crystals in a fine-grained, recrystallised matrix of quartz, plagioclase, biotite, muscovite and K-feldspar. Zircon ages yield values of 468 to 495 Ma (Valverde Vaquero and Dunning, 2000; Díez Montes, 2007; Montero et al., 2007; Bea et al., 2007). In the Puna region, the original magmatic features remain mostly unmodified by later deformational and/or metamorphic events. Here, the FMR are observed at a N–S trending domain, the Eastern Puna eruptive belt (Fig. 1b), with a length of more than 600 km. Blue quartz and plagioclase (An_{10}) phenocrysts, and K-feldspar megacrysts (≤10 cm) are included in a recrystallised, fine-grained matrix composed of quartz, alkali feldspar, biotite, muscovite and sericite (Fig. 2). Age ranges from 460 to 490 Ma according to radiometric absolute determinations (Viramonte et al., 2007).

Fig. 3 and Table 1 show the main geochemical features of these FMR. The identity in geochemical features and age of these igneous sequences in South America and Iberia, as well as the position of both zones at the Western Gondwana continental margin during Cambrian times, indicate that they formed part of the same magmatic event (Fernández et al., 2008). In both geological domains FMR show high silica contents, typical of dacite to rhyolite compositions. They are slightly peraluminous and rich in alkalis. However, they show more than twice the Fe and Mg contents of normal silicic magmas, and less than half the Ca content of magmatic rocks with similar Fe and Mg contents. The large homogeneity of FMR across several km thick volcanic and volcanoclastic sequences, together with a limited range

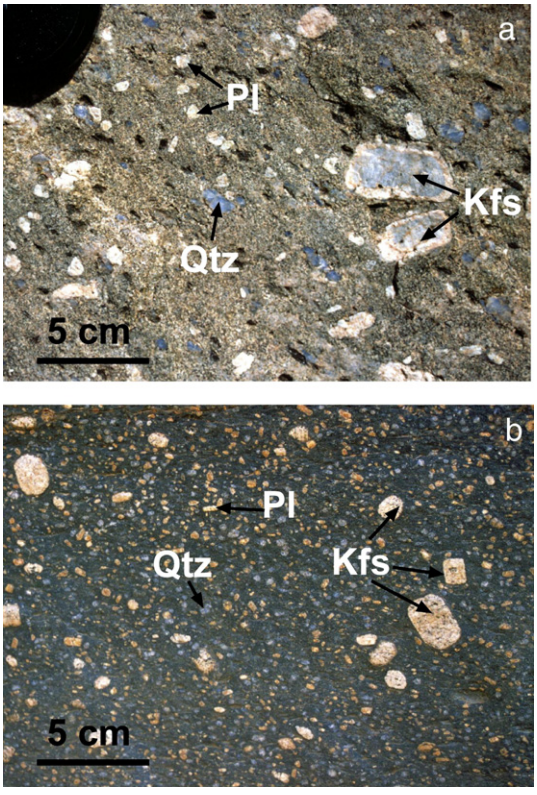

Fig. 2. Photographs showing textural features of the FMR from the Puna eruptive belt (Argentina). Note the phenocryst assemblage formed by K-feldpsar, albitic plagioclase and quartz (blue), enclosed in a fine-grained dark matrix. (For interpretation of the references to colour in this figure legend, the reader is referred to the web version of this article.)

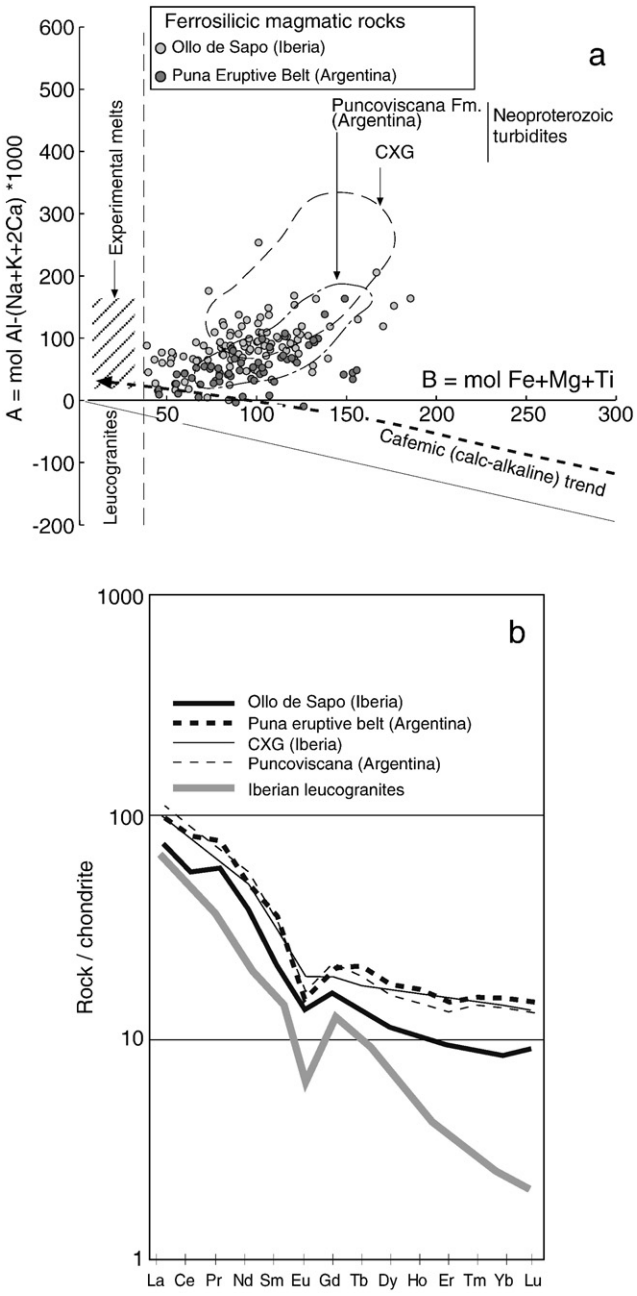

Fig. 3. Main geochemical features of the Cambro-Ordovician magmatic rocks of Iberia (Ollo de Sapo formation) and Puna Eruptive belt (Argentina). (a) Major element features shown in multicationic diagrams A–B (Debon and Le Fort, 1983). Note the slightly peraluminous character of the FMR, in part overlapping the field of the Neoproterozoic turbidites (metagreywackes) from the same geological domains, namely the Puncoviscana formation in South America and the Schist and Greywacke Complex (CXG, Compleixo dos Xistos e Grauvacas) in Iberia. Leucogranites and low melt fraction experiments from metagreywackes (e.g. Montel and Vielzeuf, 1997, Castro et al., 1999) plot out of the field of ferrosilicic rocks. (b) Comparison of average REE patterns. Note the depletion in HREE observed in the Ollo de Sapo ferrosilicic rocks compared to the Neoproterozoic turbidites (CXG). This depletion is not observed in the ferrosilicic rocks from The Puna Eruptive Belt compared to the Puncoviscana metagreywackes. Strongly fractionated anatectic leucogranites (low melt fractions) are plotted for comparison (see Fernández et al., 2008, for data compilation).

Table 1
Average major element compositions of ferrosilicic magmatic rocks and metagreywackes from Puna and Iberia and starting materials used in experiments.

	Ollo Iberia (1)		Puna E. Belt (1)		CXG Iberia (1)		Puncoviscana (1)		HR-40 (2)	VSOS (3)
	Average ($n=95$)	S.D.	Average ($n=59$)	S.D.	Average ($n=68$)	S.D.	Average ($n=13$)	S.D.		
SiO2	67.53	*2.81*	69.12	*2.51*	64.16	*7.16*	70.40	*5.17*	67,85	70,30
TiO2	0.55	*0.18*	0.60	*0.21*	0.84	*0.23*	0.71	*0.11*	0,91	0,53
Al2O3	15.79	*1.21*	14.64	*0.85*	17.64	*3.79*	13.22	*2.70*	17,17	15,46
FeOt	3.77	*1.03*	3.84	*1.05*	6.08	*1.57*	4.54	*1.03*	6,01	3,84
MgO	1.56	*0.57*	1.62	*0.55*	2.12	*0.62*	1.93	*0.43*	2,27	1,54
MnO	0.04	*0.02*	0.07	*0.02*	0.04	*0.03*	0.08	*0.02*	0,04	0,04
CaO	1.19	*0.51*	1.63	*0.84*	0.27	*0.23*	0.93	*0.43*	0,50	1,30
Na2O	2.86	*0.58*	2.81	*0.50*	1.55	*0.77*	2.38	*0.46*	2,35	3,11
K2O	4.18	*0.73*	4.02	*0.86*	3.43	*1.12*	2.86	*1.07*	2,90	3,88
P2O5	0.17	*0.07*	0.19	*0.06*	0.15	*0.09*	0.17	*0.05*		
L.O.I.	1.90	*0.74*	1.07	*0.46*	1.63	*1.98*	2.46	*0.70*		
Total	99.80		98.88		98.03		96.89		100	100

(1) According to data compilation in Fernández et al. (2008); (2) Synthetic anhydrous glass from greywacke HR40 (Ugidos et al., 1997); (3) Synthetic anhydrous glass of ferrosilicic composition. *n* is number of samples and S.D. the standard deviation.

of silica (65–70 wt.% SiO2) and the scarcity or null presence of mafic compositions in the sequence, point out to FMR as primary magmas, not derived by igneous fractionation from any parental, more mafic magma. Furthermore, FMR have strong chemical similarities with regionally related Neoproterozoic metagreywackes (Schist and Greywacke complex in Iberia and Puncoviscana formation in Puna, Fig. 1). The average chemical compositions of these metagreywackes and FMR are shown in Table 1. Details on the geochemical comparisons between ferrosilicic magmas and metagreywackes are given in a separate paper (Fernández et al., 2008). In the A–B diagram (Fig. 3a), the FMR plot in the peraluminous field (A>0) with values of B (ferromagnesian components) comprised between 50 and 150. This plotting area is restricted to greywacke sediments, rich in Fe and Al, as it is expected from weathering fractionation process in which clay minerals concentrate Fe, Al, Mg and K, and Ca is lixiviated in water solution (Taylor and McLennan, 1985). Furthermore, they plot out of the cafemic (calc-alkaline) trends (Fig. 3a) and the field of partial melts (leucogranites) derived by low melt fractions of metagreywacke sources (Montel and Vielzeuf, 1997; Castro et al., 1999). Comparisons in REE between metagreywackes and FMR are shown in Fig. 3b. Only a slight depletion in HREE is observed for the Iberian FMR. In summary, we are dealing with a particular case of primitive magmas that have a composition out of calc-alkaline trends and almost coincident with the metagreywacke field (Table 1).

3. Ferrosilicic magmas: liquids or restite-melt systems?

In a previous paper (Fernández et al., 2008), we have shown independent evidences, including rock geochemistry and high temperature melting experiments, that strongly support the derivation of ferrosilicic magmas by near-total melting (melt fraction >0.8) of metagreywackes or their deep equivalents, including potential charnockitic rocks. It was established that temperatures higher than 1000 °C are necessary to produce such high melt fractions. Lower melt fractions may give rise to ferrosilicic magmas if Fe- and Mg-rich restites are dragged from the source together with the leucogranite melt. Mass balance calculations indicate that more than 70 wt.% of restite is needed to account for the Fe and Mg content of the ferrosilicic rocks. Thus, it is important to determine if these FMR derived from crystallisation of a Fe- and Mg-rich melt or, on the contrary, they represent mixtures of melts and Fe- and Mg-rich restites dragged from the source. In the latter case, the temperature needed for magma generation is lower by about 300 °C than that required for the generation of a Fe- and Mg-rich melt.

Observation of anatectic areas shows that leucogranite melt is segregated in veins and plutonic bodies leaving a residue rich in Fe and Mg at depth. In the case of the FMR, a near-total mobilization of the solid residue is needed to account for the observed composition. The observed similarities in the REE patterns between FMR and metagreywacke sources (Fig. 3b) preclude any selective enrichment in Grt. Instead, the slight depletion in HREE may indicate that some Grt has been left in the source. A restite-melt system as that required in this case, with a crystal content of about 70 vol.%, has a rheological behaviour similar to a solid rock (e.g., Vigneresse et al., 1996), very unlike to flow and be emplaced at shallow crustal levels or be erupted to the surface. The eruption probability for silicic magmas is maximized at 30–40 vol.% of crystals. It strongly decreases for crystallinity larger than 60 vol.% (Marsh, 1981). These observations support that the FMR represent melt compositions and not mixtures of low-temperature melt plus restite. In addition to these rheological limitations, textural observations are indicative of crystallisation from a Fe-rich melt.

The phenocryst assemblage of the FMR is dominated by quartz, plagioclase and K-feldspar (Fig. 2). There is no evidence for the presence of restitic phases, either as phenocrysts or matrix. The large proportions of restite needed to account for the Fe and Mg content is incompatible with the typical volcanic textures observed in these

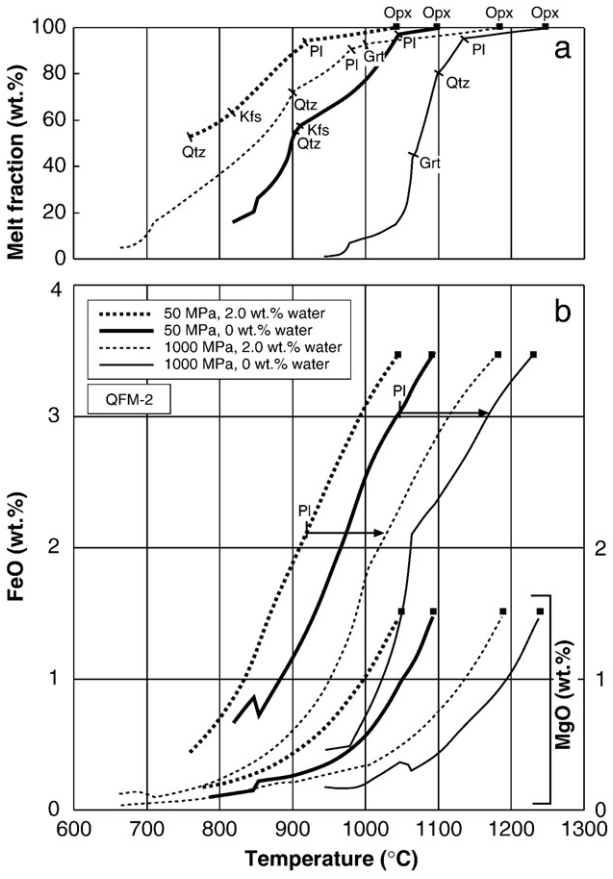

Fig. 4. (a) Temperature vs melt fraction and (b) Fe, Mg saturation curves for wet and dry ferrosilicic melts with FeO = 3.5 wt.% and MgO = 1.5 wt.% (Table 1) calculated by MELTS algorithm at 50 MPa and 1.0 GPa. Liquidus temperatures are ca. 150 °C higher at high pressure. Low-pressure crystallisation (shallow magma chamber) of Pl starts at about 950 °C in equilibrium with a wet melt (2.0 wt.% water) and at about 1080 °C for a dry melt. These T are more than 100 °C at higher pressure (segregation). Assuming adiabatic ascent, a first estimate of temperature source region (1.0 GPa pressure) is ca. 1200 °C and 1020 °C for dry and 2.0 wt.% water, respectively. These values are minimum assuming a pressure of generation of 1.0 GPa. Pressure may be higher (1.5 GPa), according to additional constraints given in the text. Note that the liquidus phase is Opx with independence of pressure and water content.

rocks (Díez Montes, 2007). Textural observations are particularly relevant in the case of the Puna rocks where no metamorphic or tectonic process modified the original magmatic mineralogy (Fig. 2). The phenocryst assemblage may have been developed in a shallow magma chamber connected to eruptive vents. Also, the less deformed and metamorphosed facies of the Iberian Ollo de Sapo formation show textures indicating lavic, pyroclastic, and epiclastic provenances (Díez Montes, 2007). Euhedral quartz and feldspar phenocrysts are key features of the lavic rocks. Quartz phenocrysts show rounded embayments including partially a fine-grained groundmass. Euhedral crystals of albitic plagioclase are free of inclusions. These are identical to inclusions in the large K-feldspar phenocrysts (up to 10 cm length, Fig. 2) that characterize these FMR. The inference that high temperature (>1000 °C) and melt fraction (>50 vol.%) are needed for the generation of these magmas from a metagreywacke source is compatible with a high temperature of crystallisation in a shallow magma chamber.

3.1. Temperature of crystallisation of ferrosilicic melts

The observed positive correlation between the liquidus temperature and Fe–Mg content in granitic systems (Johannes and Holtz, 1996) may be used here as a first-order approach to determine magma temperatures. Saturation of Fe and Mg for a silicic melt with the composition of the FMR has been calculated for equilibrium crystallisation using the MELTS algorithm (Ghiorso and Sack, 1995; Asimow and Ghiorso, 1998). The results are shown in Fig. 4. The liquidus phase of this system is orthopyroxene (Opx) at appropriate pressure. Since this phase is a Fe–Mg saturating phase, the curves shown in Fig. 4 can be considered the solubility curves. The low-pressure phase relations, simulated by MELTS, are in agreement with the observed pre-eruptive/intrusive phenocryst assemblage dominated by quartz (Qtz) and feldspar, with subordinate Opx and devoid of Grt. The inference from these relations is that most of Fe and Mg contents of the magma system were dissolved in the melt at the time of crystallisation of Qtz and feldspars. Dry and water-undersaturated (2.0 wt.% water) conditions are compared in these diagrams. The Fe content of the melt at the temperature of plagioclase (Pl) saturation (1050 °C) is about 3.0 wt.% FeO in dry ferrosilicic magma. For a wet magma, the Fe content of the melt is about 2.2 wt.% FeO at the temperature of Pl saturation (ca. 920 °C). The equilibrium temperature at the pressure of melt generation and segregation, here calculated at a minimum pressure of 1.0 GPa (Fig. 4), is up to 100 °C higher than at shallow conditions of 50 MPa. In both cases, dry and wet systems, the melt fraction at the temperature of Pl saturation is about 0.9 (90 wt.% melt). Minimum temperatures of about 900 °C were determined by the Ti-in-zircon thermometer (Watson et al., 2006) in magmatic overgrowths of Cambro-Ordovician age, representing the minimum temperature of magma crystallisation in the crust (Bea et al., 2007) for these ferrosilicic magmas. This temperature is in agreement with the above mentioned phase relations and phenocryst assemblage, implying a peculiar melt composition with high Fe and Mg contents. Inverse experiments are used here to test these model predictions for ultrahigh temperature.

4. Inverse experiments

Near-liquidus phase relations for a model composition representative of the ferrosilicic magmatic rocks are explored here in detail. Based on the inferences for the liquid nature of the studied magmatic rocks at the time of segregation and the requirements for high melt fractions from a metagreywacke source, previously determined experimentally (Fernández et al., 2008), we have designed a set of crystallization experiments (inverse experiments) aimed to determine the coexisting assemblages obtained at variable conditions of pressure and temperature. The starting material is a synthetic glass with the average composition of ferrosilicic magmatic rocks found in Iberia and Puna belts (VSOS, Table 1).

4.1. Experimental procedures and analytical techniques

A synthetic glass has been used for experiments aimed to determine the near-liquidus phase relations (Table 1). Pure oxides were mixed at room temperature with Na and K silicates in the desired proportions. Iron is added in the form of ferric oxide. After mixing for half an hour in an acetone medium, the homogeneous mixture is introduced in small portions in a graphite crucible inside a vertical-loading furnace previously set at 1500 °C. The time for melting is estimated after trial and error repeated charges. A critical time of 30 s is applied. This is the minimum time required for the partial reduction of ferric to ferrous iron and enough to produce complete melting without the formation of metallic iron, for a fixed amount of oxide-silicate mixture. After melting for 30 s, the crucible is extracted and cooled with Ar gas. The resulting glass bled is broken and checked under a binocular lens. Only bleds showing a dark green colour and lacking iron inclusions were selected. After several runs, selected bleds were milled and homogenised for half an hour in an agate mortar within an acetone medium. Because the synthesized glasses are highly hydroscopic, capsules filled with these starting materials were set in an oven at 100 °C for 24 h before sealing and introduction in the piston-cylinder. Natural rocks were also used in some experiments. However, the use of synthetic glasses is preferred in this study, particularly for completely dry systems. Natural rocks contain a significant amount of water in micas and chlorite (see Table 1). The used of these natural systems is preferred for experiments with low water content.

However, the presence of either low-grade assemblages dominated by chlorite or medium-grade assemblages dominated by biotite and muscovite, determine the amount of water in the system, and this is critical for the determination of near-liquidus relations. To avoid these inconveniences, we have used synthetic glasses for magma and source starting materials. In addition, calculations using MELTS indicate that the studied magmatic rocks were derived from a dry melt, and the optimal procedure to model a dry melt is a dry synthetic glass.

Experiments were carried out in end-loaded, Boyd-England piston-cylinder apparatus at the University of Huelva. Metal capsules containing 10 mg of sample (either rock powder or synthetic glass) are embedded in a pressure container of crushable magnesia. The reported pressures are oil pressures measured with electronic DRUCK PTX 1400 pressure transmitters, feeding OMRON E5CK controllers, multiplied by ratio of ram-to piston areas, and were manually maintained within ±5 bar of oil pressure (ca. 250 bar on the sample). Temperatures were measured and controlled with Pt100–Pt87Rh13 thermocouples feeding Eurotherm 808 controllers with internal ice point compensators. Temperature stability during all runs was ±5 °C. A NaCl sleeve with an inner glass protector is used for insulation. The resulting 1/2 in. diameter assembly is introduced into the CW pressure vessel and submitted to the desired run conditions. It has been demonstrated (Patiño Douce and Beard, 1996) that the graphite-based cell assemblies used in these experiments limit the fO_2 in the samples to a well defined interval below the QFM buffer (between QFM and QFM-2). The stability and compositions of ferromagnesian phases are not affected by fO_2 variations within the range imposed by these cell assemblies (Patiño Douce and Beard, 1996), and these fO_2 conditions are reasonable for deep crustal processes.

Gold capsules were used for experiments at temperatures up to 1050 °C and AuPd capsules for higher temperatures. Run durations have been set within critical values between the minimum rime required to reach equilibrium and a maximum time to avoid Fe loss to the capsules or water loss in the case of Au capsules. We have check

that durations on the order of 20 h are sufficient to get equilibrium and to avoid discernible Fe loss in runs at 1200 °C. Shorter durations are needed to reach equilibrium in water-added runs at temperatures of 900 to 1100 °C. In this study we consider that equilibrium was reached if melt composition is homogeneous, with standard deviations within WDS analytical errors of about 5% relative. Also the lack of significant compositional zoning in new-formed minerals is considered as a criterion of equilibrium. After run, the experiments were quenched by cutting-off the power. A fast dropping of temperature with rates of about 100 K/s is obtained, minimizing the formation of quenching minerals. Al-silicate needles formed by quenching were observed in few cases. A fast heating ramp of 100 K/min (the maximum allowed by the Eurotherm 808 controller) was applied to all experiments in order to avoid the formation of metastable phases during heating. However, metastable phases may have developed in some experiments (see below). Capsules were checked for tears, mounted in epoxy and half cut with a diamond disk, for examination with the SEM and EPMA. Mineral and melt proportions were determined by image analyses of back-scattered electron (BSE) images (Z-contrast) with ImageJ software. Chemical compositions of minerals and melts (glasses) were determined by WDS with a JEOL JXA 8200 Superprobe equipped with four WDS channels at the University of Huelva. A combination of silicates and oxides were used as standards for calibration. Operating conditions were 15 KV accelerating voltage and 15 nA probe current. A defocused beam of 30 μm was used for glass analyses in order to minimize Na loss. Only in cases of small melt pools in low melt fraction experiments, a normal smaller beam of 3 to 10 μm was used to avoid contamination with X.-rays from the surroundings. In these cases, a significant Na loss of about 30 to 50% relative was observed.

4.2. Results from inverse experiments on the ferrosilicic system

Inverse experiments using the VSOS synthetic glass (Table 1) were performed to help to constrain the PT conditions of near-total melting and to constraint the stability field of Grt in the source region. Average values from microprobe point analyses from glasses and minerals are given in Table 2 (runs 1 to 6). The following points can be remarked.

(1) Grt is a dominant phase in experiments at conditions far from the liquidus. Opx is always present in near liquidus experiments
(2) The characteristic diagnostic phases of ultra-high temperature metamorphism of pelites (e.g. Harley, 2004) are present in runs at T>1000 °C. These are corundum (Cor), Spinel (Spl), Al-silicates (Als), and Opx. It is noteworthy the formation of Qtz as part of the coexisting assemblage with Cor, Spl and Opx in the runs at 1100 and 1200 °C. However, the coexistence of Cor and Qtz is problematic, as discussed below.

Table 2
Assemblages and phase compositions (*) of experimental runs of this study.

Run	Ref.	Sample	P (GPa)	T (°C)	wt.% Water	Duration (h)	Assemblage (vol.%) (**)	Phase	*n*	SiO_2	TiO_2	Al_2O_3	FeOt	MgO	MnO	CaO	Na_2O	K_2O	P_2O_5	Total	100–total
1	IK07-3	VS-OS	1.7	950	<1	119	Melt (5), Qtz (44) Fsp (40), Bt (8), Grt (3)	Melt	9	73.94	0.31	16.84	1.66	0.47	0.01	1.02	2.27	3.45	0.03	100	13.32
								s.d.		*1.09*	*0.02*	*0.28*	*0.07*	*0.01*	*0.02*	*0.02*	*0.61*	*0.75*	*0.01*		
								Grt	3	39.45	1.15	22.11	20.67	13.02		3.23	0.63			100	
								s.d.		*0.38*	*0.13*	*0.18*	*0.04*	*0.13*		*0.20*					
								Fld	7	64.22		21.44				3.15	7.41	3.97		100	
								s.d.		*0.47*		*0.38*				*0.24*	*0.32*	*0.39*			
								Bt	3	39.25	5.62	17.11	12.36	11.08			1.06	9.45		95.92	
								s.d.		*0.29*	*0.10*	*0.22*	*0.24*	*0.48*			*0.06*	*0.17*			
2	AC07-11	VS-OS	1.4	1000	20	14	Melt (92), Opx (8)	Melt	3	70.39	0.59	16.37	3.31	0.52	0.00	1.62	2.90	3.96	0.05	100	EDS
								s.d.		*0.63*	*0.11*	*0.47*	*0.08*	*0.52*	*0.01*	*0.04*	*0.37*	*0.09*			
								Opx	5	49.67	0.21	8.13	22.84	18.32		0.33	0.37	0.35		100	
								s.d.		*1.99*	*0.17*	*0.69*	*1.17*	*0.63*		*0.05*	*0.38*	*0.12*			
3	IK07-2	VS-OS	1.9	1000	0	70	Melt (8). Qtz (44) Fsp (29). Grt (19) Als (<1)	Melt	7	72.64	0.35	16.63	1.87	0.40	0.00	1.14	2.94	4.01	0.02	100	13.79
								s.d.		*1.24*	*0.02*	*0.23*	*0.14*	*0.02*	*0.01*	*0.05*	*0.72*	*0.79*	*0.01*		
								Fsp	5	64.46		21.48	0.33			2.76	6.64	5.34		100	
								s.d.		*0.25*		*0.45*	*0.00*			*0.36*	*0.32*	*0.81*			
								Grt	4	39.59	1.11	22.11	20.07	12.88	0.38	3.65				100	
								s.d.		*0.36*	*0.25*	*0.18*	*0.89*	*0.38*	*0.02*	*0.18*					
4	IK07-4	VS-OS	1.7	1050	0	118	Melt (13), Qtz (30) Fsp (50), Grt (7) Opx (<1)	Melt	8	73.94	0.31	16.84	1.66	0.47	0.01	1.02	2.27	3.45	0.03	100	14.90
								s.d.		*1.09*	*0.02*	*0.28*	*1.72*	*0.47*	*0.02*	*0.02*	*0.61*	*0.75*	*0.01*		
								Fld	3	63.05		22.78		0.46		4.49	7.55	2.13		100	
								s.d.		*0.54*		*0.62*		*0.01*		*0.37*	*0.30*	*0.33*			
								Opx	3	*48.46*	*0.43*	*3.28*	*26.89*	*17.50*		*0.66*				97	
								s.d.		*0.33*	*0.11*	*0.10*	*3.70*	*0.30*		*0.13*				5	
								Grt	3	*39.45*	*0.98*	*22.18*	*18.67*	*15.14*		*2.75*				99	
								s.d.		*0.40*	*0.24*	*0.30*	*0.38*	*0.41*		*0.06*					
5	AC07-31b	VS-OS	1.6	1100	0	42	Melt (38), Qtz (37) Pl (15), Opx (10) Cor + Spl (<1)	Melt	5	68.42	0.95	16.11	3.48	0.56	0.01	0.83	4.51	5.11	0.02	100	3.42
								s.d.		*0.56*	*0.42*	*1.09*	*1.54*	*0.29*	*0.01*	*0.02*	*1.12*	*0.22*	*0.01*		
								Pl	3	*65.53*		*20.25*				*1.42*	*6.71*	*6.01*		99	
								s.d.		*0.24*		*0.71*				*0.57*	*0.45*	*0.78*			
								Opx	3	*48.46*		*3.27*	*29.22*	*17.50*		*0.66*				99	
								s.d.		*0.33*		*0.09*	*0.54*	*0.30*		*0.13*					
								Spl	3			*57.63*	*33.75*	*8.63*						100	
												0.84	*1.21*	*0.63*							
6	AC07-21	VS-OS	1.5	1200	0	14	Melt (75), Qtz (10) Spl (10), Cor (5)	Melt	4	68.21	1.21	15.89	4.49	1.31	0.02	0.95	4.01	3.91	0.03	100	3.19
								s.d.		*0.94*	*0.14*	*0.52*	*0.48*	*0.26*	*0.02*	*0.11*	*0.18*	*0.48*	*0.01*		

n. number of point analyses; s.d. Standard deviation.
(*) WDS probe analyses excepted those labelled with EDS. Opx, St and Spl analyses are only approximate due to the small size (<2 μm) of crystals. Missing analyses due to crystal sizes of less than 1 μm. (**) Modal estimations by image analysis on BSE images.

(3) The melt fraction is about 75 vol.% at 1200 °C for dry conditions. Grt is absent in these runs at 1200 °C.
(4) The system is close to the liquidus at 1000 °C (92 vol.% melt) and 1.4 GPa in excess water. Opx is the only coexisting phase in this run.
(5) At 1100 °C and 1.6 GPa, Grt is present in the coexisting assemblage with only 35 vol.% melt.

Results from the inverse experiments inform that Opx is the liquidus phase of the ferrosilicic system at any pressure and water content. The crystallisation of Grt requires lower temperatures, about 100 °C below the liquidus with independence of the water content. The high FeO content of the melt at high pressure is in agreement with conditions near the liquidus of the system, where Grt is absent. The implication is that ferrosilicic magmas represent near-liquid systems that were segregated form the source before Grt crystallisation. The final cooling at pre-eruptive, shallow magma chambers took place at conditions out of the stability field of Grt, as mentioned above. This is apparently in contradiction with the inference from REE depletion relating fractionation of Grt. This suggests that Grt is a residual restitic phase formed in the course of melting reactions of the metagreywacke source and not a phase crystallised from the ferrosilicic melt. Conditions for melt generation in the presence of Grt were reported in a previous experimentsal study (Fernández et al., 2008) using several model metagreywackes.

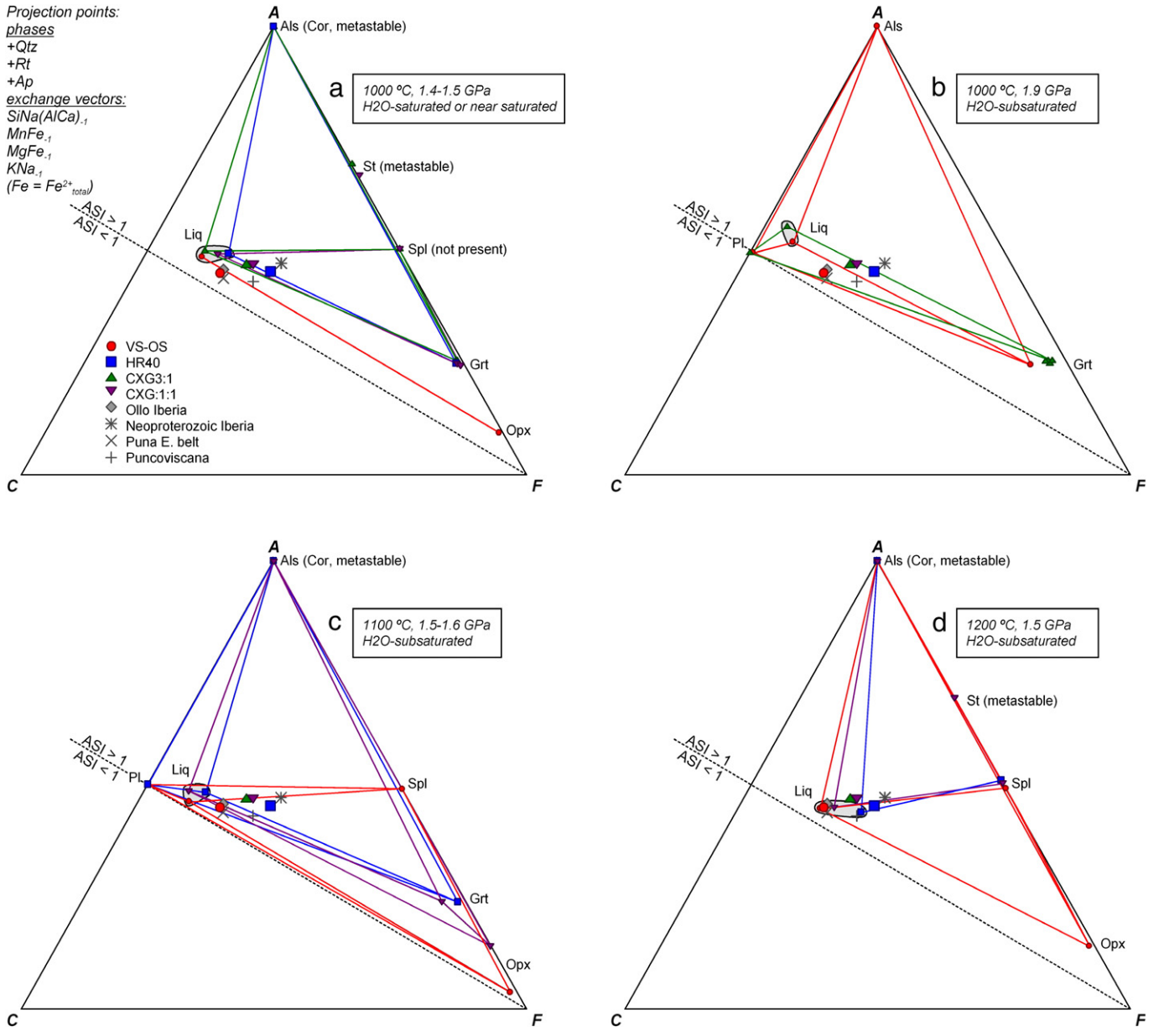

Fig. 5. De-luxe ACF diagram showing basic phase relations of near-liquidus experimental runs with the VSOS synthetic glass projected from quartz, rutile and apatite and condensed after projection from the indicated exchange vectors (this may cause crossing of tie-lines). Phase compositions from the melting experiments with metagreywackes (HR40, CXG3:1, CXG1:1) (Fernández et al., 2008) are also included for comparisons in these diagrams. a) Experiments at 1000 °C, 1.4–1.5 GPa, 10–20 wt.% added water. b) Experiments at 1000 °C, 1.9 GPa, 0.2 wt.% added water. Note that plagioclase is present and liquid is poorer in Fe–Mg relative to water-saturated conditions at 1000 °C. c) Experiments at 1100 °C, 1.5–1.6 GPa, 0–2 wt.% added water. d) Experiments at 1200 °C, 1.5 GPa, 0.2 wt.% added water. Note that bulk compositions plot adjacent to the corresponding Liq-Grt tie-lines, indicating large modal amounts of these phases. As temperature and melt fraction increase the composition of melt approaches the bulk composition. In all diagrams, corundum and staurolite are considered as metastable products relative to stable Al-slicate and spinel, respectively (see text). All projections made by using CSpace software (Torres-Roldán et al., 2000). Mineral abbreviations from Kretz (1983).

4.3. Attainment of equilibrium and the role of possible metastable phases

Systematic variations in the coexisting assemblages and the composition of melts with increasing temperature and/or water content are indicative of chemical equilibrium. It can be appreciated in the diagrams of Fig. 5 that important changes occur in the melt compositions in parallel with changes in the coexisting assemblages and physical conditions. The experimental results (melt compositions, melt fractions and coexisting assemblages) are in good agreement with simulations by MELTS algorithm.

A test for attainment of equilibrium in these experiments is given by the systematic variations of solid solutions with intensive variables. Through the ACF phase diagrams of Fig. 5 (see also Table 2), it can be appreciated that phase assemblages change systematically upon changing P–T, bulk composition and amount of water. At low temperature and low water content (1000 °C, Fig. 5b) plagioclase is present in the assemblages made of Liq + Grt + Pl ± Als. With increasing water content at the same temperature (1000 °C, Fig. 5a), plagioclase is lost, the melt fractions increase, the compositions of melt approach that of the respective systems, and Opx appears in VSOS. The latter effect is due to the relatively high "C" content of VSOS (i.e., it plots closer to feldspar) that makes possible the Opx – Pl tie-line (note that bulk composition plots adjacent to this tie-line). In bulk compositions with lower "C" component the assemblage is made of Grt + Als ± Cor ± St + Liq. However, the bulk compositions plot adjacent to the Grt-Liq tie-lines, indicating high modal amount of these phases and negligible modal amounts of other phases. Upon increasing temperature at low water contents (1100 °C, Fig. 5c) bulk composition VSOS (with higher "C" component) is made of Liq – Grt – Opx – Pl – Spl whereas samples with lower "C" component are made of Liq – Grt – Pl – Als/Cor ± Opx. At still higher temperature (1200 °C, Fig. 5d) plagioclase and garnet disappear in all bulk compositions, Spl is ubiquitous and Opx is present only in bulk composition VSOS. The melt fractions increase and the compositions of melt closely approach the respective bulk compositions. To be noted is that, for the P–T–H_2O window investigated, the stability of Opx is strongly influenced by bulk composition, as indicated by its persistence in bulk composition VSOL bearing the highest "C" component. On the other hand, the presence of garnet is systematic in all bulk compositions at temperature lower than 1200 °C, suggesting that its stability is mostly controlled by temperature, in agreement with theoretical predictions as calculated by MELTS.

The composition of melt is controlled by physical conditions and bulk composition. At high temperature when the melt fractions approach 1 the composition of the melts are peraluminous, as expected from the peraluminous composition of all bulk compositions investigated. At low temperature, the melts have a stronger peraluminous character, suggesting that melts formed at the solidus of the systems investigated are strongly peraluminous. This feature is important to explain the moderate peraluminous character of the ferrosilicic magmatic rocks studied here and the crystallization of peraluminous phases such as biotite.

In a number of experiments corundum and quartz appear as coexisting phases. Experimental evidence and thermodynamic calculations suggest that the assemblage corundum + quartz is not stable with respect to kyanite or sillimanite (e.g., Harlov and Milke, 2002). According to the Ostwald step rule, it should be easier to nucleate corundum in a first step and aluminosilicate in a second step. This would imply that the assemblage corundum + quartz is metastable with respect to sillimanite/kyanite + quartz. Thus, we interpret the development of the former assemblage in our experiments as a metastable equilibrium feature. The metastable formation of corundum, however, would have little impact in the composition of coexisting phases, notably the melt, as far as the amount of these phases formed in all experiments is very small (and the amount of melt is large to very large).

5. Discussion

5.1. Magma source and melting conditions

The results of this experimental study strongly support that the ferrosilicic magmatic rocks derived from crystallization of a high temperature ferrosilicic melt. The estimated conditions of pressure and temperature are in agreement with the previous results of forward experiments using metagreywackes as starting materials (Fernández et al., 2008). In both geological domains where these rocks have been studied, the Argentinian Puna and the Iberan massif in Spain, Neoproterozoic greywacke sediments are widely represented by the Puncoviscana formation and the Schist and Greywacke complex respectively. The most relevant geochemical fingerprints of this peculiar magmatism were inherited from these sedimentary formations. These huge turbiditic successions were the final results of the changes that affected the Earth during the Neoproterozoic (Maruyama and Santosh, 2008; Rino et al., 2008; Stern, 2008; Meert and Lieberman, 2008; Komiya et al., 2008). The identification of a large population of zircon inheritances (Montero et al., 2007; Bea et al., 2007) with the age of the Neoproterozoic metagreywackes (ca. 610 Ma) is an important proof for the source of magmas. This fact, together with the strong similarities in trace elements, particularly in REE, as well as in radiogenic isotopes (Fernández et al., 2008), is an indicator of magma provenance. These aspects do not report, however, on the melting process or melting conditions. Peraluminous leucogranites that are derived by low melt fractions from the same magma source during the Variscan orogeny (340 to 300 Ma) are strongly fractionated in major and trace elements with respect to the source (e.g. Bea, 1991). Fractionation, however, is very limited in the Cambro-Ordovician FMR upon being derived from the same source to the Variscan leucogranites. A high melt fraction is required to transfer the geochemical signatures, especially those based in major elements. Melt fractions of 30 to 50 vol.% were obtained at 1000 °C in previous studies (Castro et al., 1999) with similar starting materials. However, the composition of melts is far from that of the ferrosilicic magmatic rocks, for which higher melt fractions and, consequently, higher temperatures are required. The results from the near-liquidus experiments shown here clearly indicate that ultra-high temperatures (>1000 °C) are required with independence of pressure or water content.

The effect of water in the melting process is determined by analysis of phase relations in a T–X_{water} section for a metagreywacke system, representing the source of ferrosilicic melts, at 1.5 GPa and fO_2 = QFM-2 (Fig. 6). Upper and lower temperature boundaries are traced. These are the minimum and maximum conditions required for the generation of Fe-rich melts (FeO = 4.0 wt.%) in equilibrium with Grt in the source. Conditions within this range, from dry to saturated, imply melt fractions of about 90 wt.%. The line of 10 wt.% Grt shows conditions for significant HREE depletion in the system. The observed HREE depletion in the Iberian FMR (Ollo de Sapo, Fig. 3) is accounted for by fractionation of 2–6 wt.% Grt with an Yb content from 60 to 80 ppm. These values are within the range of 10–154 ppm Yb found in similar metasedimentary rocks (Bea, 1996). The inflections in the FeO curves at FeO = 4.0 wt.% (Fig. 6) correspond to the 'Grt-out' peritectic reaction (Grt = Opx + melt). To overcome this reaction, an extra increment in temperature is needed. Consequently, the 4.0 wt.% content in the melt may be the result of a thermal boundary imposed by the melting reaction.

The ideal conditions for ferrosilicic melts showing HREE depletion and equilibrium with Grt in the source region are 1.2 GPa for low Fe facies and 1.5 GPa for the most abundant facies with FeO = 4.0 wt.%. These conditions apply particularly to the ferrosilicic rocks of Iberia where the HREE depletion is more conspicuous compared with the equivalent rocks of the Puna region (see Fernández et al., 2008 for comparisons).

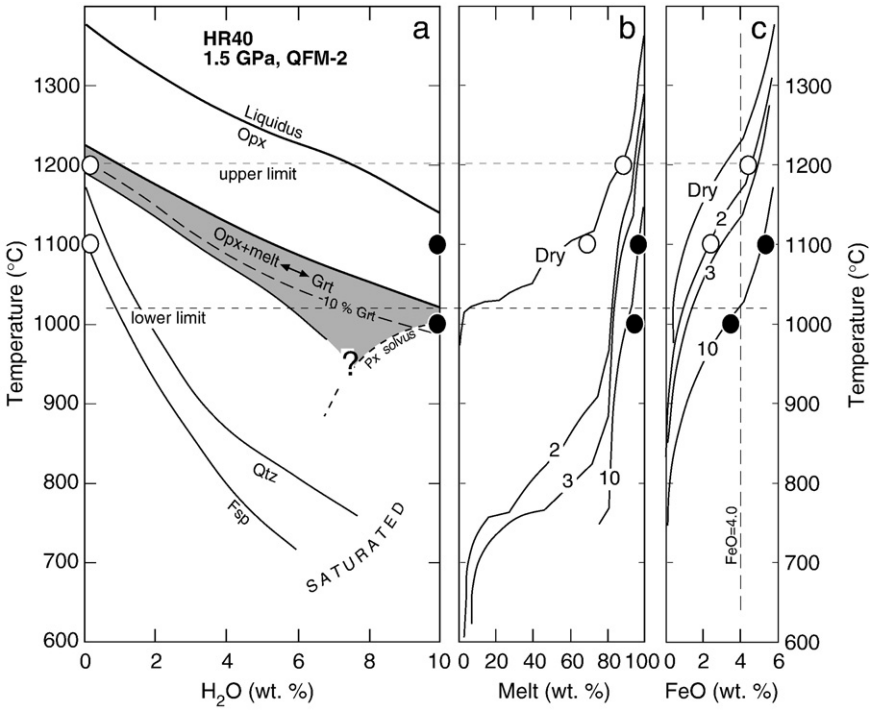

Fig. 6. a) T–X_{water} section obtained from MELTS simulations for the HR40 metagreywacke at 1.5 GPa. b) and c) show the variations of melt fractions and FeO content in the melt with temperature respectively. The curve of 10 wt.% Grt is shown within the Grt → Opx reaction band. This is indicative of Grt in the source to account for the observed HREE depletion in some FMR. Numbers on the curves in b) and c) are wt.% water. FeO contents after recasting to an anhydrous basis. Circles represent experimental runs at 1.5 GPa of HR40 metagreywacke (open circles: dry: full circles: saturated). See text for further explanations.

According to the experimental results, compositional variations observed in the ferrosilicic magmatic rocks can be attributed to variations in intensive variables, P, T and water activity rather than to the heterogeneous composition of the source. This is in agreement with the Fe and Mg solubilities resulting from thermodynamic simulations with MELTS that were exposed above (Fig. 4). The implication is that temperature was not homogeneous at the source region with important gradients of more than 200 °C within the source region. These observations will be discussed below in relation with the heat source and heating mechanisms.

5.2. Possible tectonic origin: cold silicic diapirs?

Two major problems arise to account for the near-total melting process. First, the need for a large thermal anomaly capable to reach 1000 to 1200 °C in the metasedimentary source region. Second, a closed system is needed to prevent that partial melts are segregated when they reach melt fractions of the order of 30 to 40 vol.%. At these melt fractions the rheological threshold (Vigneresse et al., 1991) is overcome, the melt has physical continuity in the system and the segregation is likely to occur. However, the process invoked according to our experimental results requires that melt remains in the source until a high melt fraction (>80 wt.%) is reached. It is well known that this is not the case of anatectic areas in the continental crust, where melts are segregated in relation to tectonic activity acting at the time of partial melting. Melt segregation at 5–10 vol.% melt is even possible at actively deforming belts (e.g., Brown and Rushmer, 1997). Consequently, partial melting with low melt fractions (5 to 30 vol.% melt) is a typical crustal process imposed by the rheology of crustal materials with contrasted compositions and strong rheological discontinuities. Furthermore, partial melting of crustal protoliths is always associated with orogenic processes, either extensional or compressional, that favour the segregation of melts via shear bands or any type of local extensional regime in response to deviatoric stresses acting on a rheologically discontinuous crustal environment. It seems very unlikely that melting fractions of the order of 70 to 90 vol.% can be produced in the continental crust, unless protected from large-scale deforming regions. The high temperatures needed for this melting process (1000 to 1200 °C) are also unlike in the continental crust.

A possible solution to this paradox is that melting occurred at the core of a cold diapir formed by subducted sediments ascending into the hot mantle wedge. The possibility for thermal-rheological instabilities that give rise to these mantle wedge mega-structures was analyzed in detail by Gerya and Yuen (2003; but see also Ernst, 2007, and Maruyama et al., 2007). The application to continental active margins was established by Gerya and Stoeckhert (2005) and Currie et al. (2007). In these models large portions of the upper continental crust (e.g. sedimentary piles) may be subducted and transported by cold diapirs to the mantle wedge, giving rise to large silicic magma chambers. Ascent of these strongly buoyant structures involves fast decompression and heating (3–1 GPa and 400–600 °C in 1–5 Ma) associated with rapid melting (Gerya and Yuen, 2003; Gerya et al., 2004; Gerya and Stoeckhert, 2005). Melting is caused by combined effects of decompression, conductive heating from the surrounding hot mantle wedge and shear heating associated with strong deformation inside and outside the plume (Gerya and Yuen, 2003). Melt segregation at low melting rates is very unlike at the core of these cold diapirs as they ascend very rapidly (centimetres to meters per year, Gerya et al., 2004) through the mantle wedge within a nearly continuous medium. Also reaction with the mantle rocks may help to preserve these mega-structures due to the formation of a reactive aureole rich in pyroxene and amphibole (Castro and Gerya, 2008). Massive subduction of previously accreted sedimentary rocks resulting in cold silicic diapir activity can be caused by sudden changes in the regime of subduction from accretion- to erosion-dominated. Such changes can be related to acceleration of subduction rate, increase in traction along the slab interface, and/or increase in strength and thickness of accreted sediments (e.g. Gerya and Yuen, 2003; Sobolev and Babeyko, 2005; Gerya and Stoeckhert, 2005; Currie et al., 2007). In order to test this scenario we performed numerical

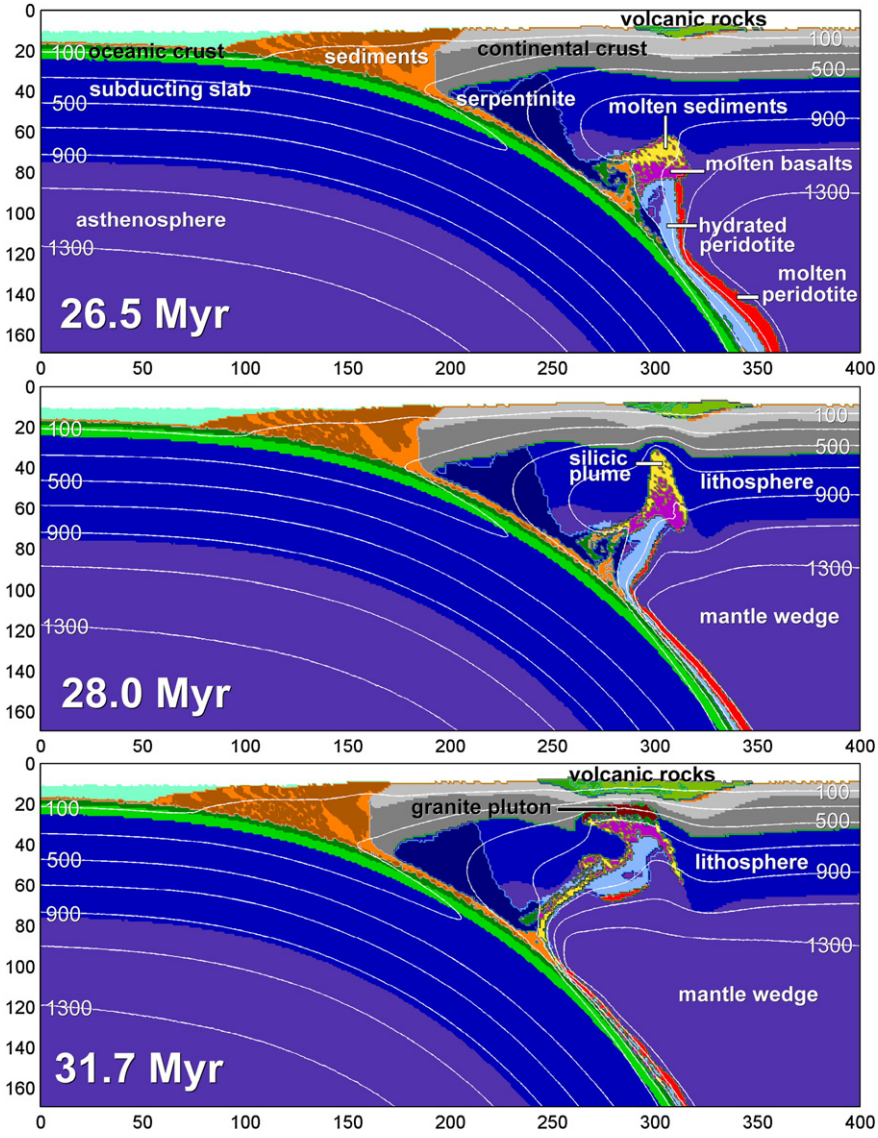

Fig. 7. Results of numerical modelling of subduction at an active continental margin associated with silicic diapir development (see Gorczyk et al., 2007 for details of model setup and numerical approach). A 40 Myr old oceanic plate subducts at a constant velocity of 5 cm/yr. The numerical model takes into account water release from the subducting oceanic crust, mantle wedge hydration, partial melting of rocks and growth of layer of volcanic rocks atop the continental crust.

simulation with the use of numerical model of subduction under a continental margin (Gorczyk et al., 2007). Results of the numerical experiment (Fig. 7, see also movie in the supplementary material) demonstrate feasibility of a diapiric scenario for the origin of silicic batholiths. Silicic plume (diapir) is composed of subducted sediments and oceanic crust subjected to melting at high temperature (900–1000 °C) at sublithospheric depths. This diapir intrudes into the lithosphere at high ascent rates (up to 40 km/Myr) and emplaces into the extending continental crust. High rates of penetration through the strong mantle lithosphere are related to rheological weakening effects due to the assumed propagation of magmatic fluids from the diapir through the network of faults forming above the ascending magmatic body (Gerya and Burg, 2007). Furthermore, the fault network generated in the extending lithosphere above the ascending diapir is able to continually extract melt from the magmatic body (Chen and Jin, 2006). This channeled melt may quickly arrive to the Earth's surface. Ascent velocity of melt inside the fracture network depends on the density difference between melt and host rock, the shear viscosity of the ascending magma and the width of the ascent conduit (Petford et al., 1993). Typical ascent velocities for dike transport of silicic magmas are in the range 0.1–0.3 m s^{-1} (Petford et al., 1993; Fernández and Castro, 1999). Therefore, the ferrosilicic melt may traverse the crust and even the whole lithosphere in less than 30 days. These fast ascending rates do not favour geochemical interaction and contamination of the ascending melt with the lithosphere mantle and the crust.

6. Conclusions

The results of inverse experiments with the model ferrosilicic composition (VSOS) indicate that conditions of 1000 °C (wet conditions) and 1100–1200 °C (subsaturated and dry) at pressures of 1.4 to 2.0 GPa are the most plausible conditions for generation. A thermal regime of this kind affecting crustal rocks can be found at the core of mantle-wedge plumes or silicic cold diapirs developed at the subduction channel and ascending through the mantle wedge. The scarcity of exotic components in the plume (e.g. basalts from the oceanic slab) is a peculiar feature of this silicic magmatism, possibly resulting from the unusually large turbiditic basins developed at the margin of the Gondwana supercontinent during Neoproterozoic and Lower Cambrian times, just predating the formation of the ferrosilicic magmatism. The incorporation of thick sedimentary sequences into

the subduction channel likely resulted in the formation of mantle-wedge plumes composed exclusively of sedimentary materials that gave rise by high degrees of melting to the ferrosilicic magmas.

Acknowledgements

This work has been supported by the Spanish Ministry of Science and Education (Projects CGL2004-06808-and CGL2007-63237).

Appendix A. Supplementary data

Supplementary data associated with this article can be found, in the online version, at doi:10.1016/j.gr.2008.12.011.

References

Allègre, C.J., Ben Othman, D., 1980. Nd-Sr isotopic relationship in granitoid rocks and continental crust development: a chemical approach to orogenesis. Nature 286, 335–341.
Annen, C., Sparks, R.S.J., 2002. Effects of repetitive emplacement of basaltic intrusions on thermal evolution and melt generation in the crust. Earth and Planetary Science Letters 203, 937–955.
Asimow, P.D., Ghiorso, M.S., 1998. Algorithmic modifications extending MELTS to calculate subsolidus phase relations. American Mineralogist 83, 1127–1131.
Bea, F., 1991. Geochemical modeling of low melt-fraction anatexis in a peraluminous system: the Pena Negra Complex (central Spain). Geochimica et Cosmochimica Acta 55, 1859–1874.
Bea, F., 1996. Residence of REE, Y, Th and U in granites and crustal protoliths; implications for the chemistry of crustal melts. Journal of Petrology 37, 521–552.
Bea, F., Montero, P., González-Lodeiro, F., Talavera, C., 2007. Zircon inheritance reveals exceptionally fast crustal magma generation processes in Central Iberia during the Cambro-Ordovician. Journal of Petrology 48, 2327–2339.
Brown, M., 1994. The generation, segregation, ascent and emplacement of granite magma: the migmatite-to-crustally-derived granite connection in thickened orogens. Earth Science Reviews 36, 83–130.
Brown, M., Rushmer, T., 1997. The role of deformation in the movement of granite melt: views from laboratory and the field. In: Holness, M.B. (Ed.), Deformation-enhanced fluid transport in the Earth's crust and mantle. Chapman & Hall, London, pp. 111–144.
Castro, A., Gerya, T., 2008. Magmatic implications of mantle wedge plumes: experimental study. Lithos 103, 138–148. doi:10.1016/j.lithos.2007.09.012.
Castro, A., Patiño Douce, A.E., Corretgé, L.G., De La Rosa, J.D., El-Biad, M., El-Hmidi, H., 1999. Origin of peraluminous granites and granodiorites, iberian massif, spain. An experimental test of granite petrogenesis. Contributions to Mineralogy and Petrology 135, 255–276.
Chen, Z., Jin, Z.H., 2006. Magma-driven subcritical crack growth and implications for dike initiation from a magma chamber. Geophysical Research Letters 33. doi:10.1029/2006G1026979.
Condie, K.C., 1997. Plate Tectonics and Crustal Evolution. Butterworth-Heinemann, Oxford.
Currie, C.A., Beaumont, C., Huismans, R., 2007. The fate of subducted sediments: a case for backarc intrusion and underplating. Geology 35, 1111–1114.
Debon, F., Le Fort, P., 1983. A chemical-mineralogical classification of common plutonic rocks and associations. Transactions of the Royal Society of Edinburgh: Earth Sciences 73, 135–149.
Díez Montes, A., 2007. La geología del Dominio Ollo de Sapo en las comarcas de Sanabria y Terra do Bolo. Laboratorio Xeoloxico de Laxe, Serie Nova Terra, vol. 34. 506 pp.
Ernst, W.G., 2007. Speculations on the evolution of the terrestrial lithosphere-asthenosphere systems. Plumes and plates. Gondwana Research 11, 38–49.
Fernández, C., Castro, A., 1999. Pluton accomodation at high strain rates in the upper continental crust. The example of the Central Extremadura batholith, Spain. Journal of Structural Geology 21, 1143–1149.
Fernández, C., Becchio, R., Castro, A., Viramonte, J.M., Moreno-Ventas, I., Corretgé, L.G., 2008. Massive generation of atypical ferrosilicic magmas along the Gondwana active margin. Implications for cold plumes and arc-magma generation. Gondwana Research 14, 451–473. doi:10.1016/j.gr.2008.04.001.
Gerya, T.V., Burg, J.-P., 2007. Intrusion of ultramafic magmatic bodies into the continental crust: numerical simulation. Physics of Earth and Planetary Interiors 160, 124–142.
Gerya, T.V., Stoeckhert, B., 2005. 2-d numerical modeling of tectonic and metamorphic histories at active continental margins. International Journal of Earth Sciences 95, 250–274.
Gerya, T.V., Yuen, D.A., 2003. Rayleigh–taylor instabilities from hydration and melting propel "Cold plumes" at subduction zones. Earth and Planetary Science Letters 212, 47–62.
Gerya, T.V., Yuen, D.A., Sevre, E.O.D., 2004. Dynamical causes for incipient magma chambers above slabs. Geology 32, 89–92.
Ghiorso, M.S., Sack, R.O., 1995. Chemical mass transfer in magmatic processes IV. A revised and internally consistent thermodynamic model for the interpretation and extrapolation of liquid–solid equilibria in magmatic systems at elevated temperatures and pressures. Contributions to Mineralogy and Petrology 119, 197–221.
Gorczyk, W., Willner, A.P., Gerya, T.V., Connolly, J.A.D., Burg, J.-P., 2007. Physical controls of magmatic productivity at Pacific-type convergent margins: new insights from numerical modeling. Physics of Earth and Planetary Interiors 163, 209–232.
Harley, S.L., 2004. Extending our understanding of ultrahigh temperature crustal metamorphism. Journal of Mineralogical and Petrological Sciences 99, 140–158.
Harlov, D.E., Milke, R., 2002. Stability of corundum + quartz relative to kyanite and sillimanite at high temperature and pressure. American Mineralogist 87, 424–432.
Johannes, W., Holtz, F., 1996. Petrogenesis and Experimental Petrology of Granitic Rocks. Springer, Berlin Heidelberg. 335 pp.
Komiya, T., Hirata, T., Kitajima, K., Yamamoto, S., Shibuya, T., Sawaki, Y., Ishikawa, T., Shu, D., Li, Y., Han, J., 2008. Evolution of the composition of seawater through geological time, and its influence on the evolution of life. Gondwana Research 14, 159–174. doi:10.1016/j.gr.2007.10.006.
Kretz, R., 1983. Symbols for rock-forming minerals. American Mineralogist 68, 277–279.
Marsh, B.D., 1981. On the crystallinity, probability of occurrence, and rheology of lava and magma. Contributions to Mineralogy and Petrology 78, 85–98.
Maruyama, S., Santosh, M., 2008. Models on snowball earth and Cambrian explosion: a synopsis. Gondwana Research 14, 22–32. doi:10.1016/j.gr.2008.01.004.
Maruyama, S., Santosh, M., Zhao, D., 2007. Superplume, supercontinent, and post-perovskite: Mantle dynamics and anti-plate tectonics on the core-mantle boundary. Gondwana Research 11, 7–37.
McCulloch, M.T., Wasserburg, G.J., 1978. Sm–Nd and Rb–Sr chronology of continental crust formation. Science 200, 1003–1011.
Meert, J.G., Lieberman, B.S., 2008. The Neoproterozoic assembly of Gondwana and its relationships to the Ediacaran–Cambrian radiation. Gondwana Research 14, 5–21. doi:10.1016/j.gr.2007.06.007.
Montel, J.M., Vielzeuf, D., 1997. Partial melting of metagreywackes, 2: Compositions of minerals and melts. Contributions to Mineralogy and Petrology 128, 176–196.
Montero, P., Bea, F., González-Lodeiro, F., Talavera, C., Whitehouse, M.J., 2007. Zircon ages of the metavolcanic rocks and metagranites of the Ollo de Sapo Domain in central Spain: implications for the Neoproterozoic to Early Palaeozoic evolution of Iberia. Geological Magazine 144, 963–976.
Parga Pondal, I., Matte, P., Capdevila, R., 1964. Introduction à la géologie de l'Ollo de Sapo, formation porphyroide anté-silurienne du Nord-Ouest de l'Espagne. Notas y Comunicaciones del Instituto Geológico y Minero de España 76, 119–153.
Patiño Douce, A.E., 1999. What do experiments tell us about the relative contributions of crust and mantle to the origin of granitic magmas? In: Castro, A., Fernández, C., Vigneresse, J.L. (Eds.), Understanding granites. Integrating new and classical techniques. The Geological Society, London, pp. 55–75.
Patiño Douce, A.E., Beard, J.S., 1996. Effects of P, f(O_2) and Mg/Fe ratio on dehydration melting of model metagreywackes. Journal of Petrology 37, 999–1024.
Petford, N., Atherton, M., 1996. Na-rich partial melts from newly underplated basaltic crust: the Cordillera Blanca Batholith, Peru. Journal of Petrology 37, 1491–1521.
Petford, N., Kerr, R.C., Lister, J.R., 1993. Dike transport of granitoid magma. Geology 21, 845–848.
Platt, J.P., England, P.C., 1993. Convective removal of lithosphere beneath mountain belts: thermal and mechanical consequences. American Journal of Science 293, 307–336.
Rino, S., Kon, Y., Sato, W., Maruyama, S., Santosh, M., Zhao, D., 2008. The Grenvillian and Pan-African orogens: world's largest orogenies through geologic time, and their implications on the origin of superplume. Gondwana Research 14, 51–72. doi:10.1016/j.gr.2008.01.001.
Sobolev, S.V., Babeyko, A.Y., 2005. What drives orogeny in the Andes? Geology 33, 617–620.
Stern, R.J., 2008. Neoproterozoic crustal growth: the solid Earth system during a critical episode of Earth history. Gondwana Research 14, 33–50. doi:10.1016/j.gr.2007.08.006.
Taylor, S.R., McLennan, S.M., 1985. The Continental Crust: Its Composition and Evolution. Blackwell, Melbourne.
Thompson, A.B., 1982. Dehydration melting of pelitic rocks and the generation of h2o-undersaturated granitic liquids. American Journal of Science 282, 1567–1595.
Torres-Roldán, R., García-Casco, A., García-Sánchez, P.A., 2000. Cspace: an integrated workplace for the graphical and algebraic analysis of phase assemblages on 32-bit wintel platforms. Computers and Geosciences 26, 779–793.
Ugidos, J.M., Valladares, M.I., Recio, C., Rogers, G., Fallick, A.E., Stephens, W.E., 1997. Provenance of Upper Precambrian–Lower Cambrian shales in the Central Iberian Zone, Spain: evidence from a chemical and isotopic study. Chemical Geology 136, 55–70.
Valverde Vaquero, P., Dunning, G.R., 2000. New U–Pb ages for early Ordovician magmatism in central Spain. Journal of the Geological Society (London) 157, 15–26.
Vielzeuf, D., Holloway, J.R., 1988. Experimental determination of the fluid-absent melting retalions in the pelitic system. Contributions to Mineralogy and Petrology 98, 257–276.
Vigneresse, J.L., Cuney, M., Barbey, P., 1991. Deformation assisted crustal melt segregation and transfer. GAC-MAC Abstract, vol. 16, p. A128.
Vigneresse, J.L., Barbey, P., Cuney, M., 1996. Rheological transitions during partial melting and crystallization with application to felsic magma segregation and transfer. Journal of Petrology 37, 1579–1600.
Viramonte, J.M., Becchio, R., Viramonte, J.G., Pimentel, M.M., Martino, R., 2007. Ordovician igneous and metamorphic units in southeastern Puna: new U–Pb and Sm–Nd data and implications for the evolution of northwestern Argentina. Journal of South American Earth Sciences 24, 167–183.
Von Huene, R., Schöll, D.W., 1991. Observations concerning sediment subduction and subduction erosion, and the growth of continental crust at convergent ocean margins. Reviews of Geophysics 29, 279–316.
Watson, E.B., Wark, D.A., Thomas, J.B., 2006. Crystallization thermometers for zircon and rutile. Contributions to Mineralogy and Petrology 151, 413–433.
Willner, A.P., Sebazungu, E., Gerya, T.V., Maresch, W.V., Krohe, A., 2002. Numerical modeling of PT-paths related to rapid exhumation of high-pressure rocks from the crustal root in the Variscan Erzgebirge Dome (Saxony/Germany). Journal of Geodynamics 33, 281–314.